$t \to cWW$ and $WW \to \bar{t}c + t\bar{c}$ in Extended Models

David Atwood

Theory Group, Thomas Jefferson National Accelerator Facility, Newport News, VA 23606, USA

Marc Sher

Physics Department, College of William and Mary, Williamsburg, VA 23187, USA

Jenkins has pointed out that the process $t \to cW^+W^-$ is GIM suppressed in the standard model. In this note, we calculate the branching ratio for a wide range of models, in which the decay occurs at tree level through exchange of a scalar, fermion or vector. In the case of scalar exchange, a scalar mass between $2m_W$ and 200 GeV leads to a resonant enhancement, giving a branching ratio as high as a few tenths of a percent. We then note that all of these models will also allow $W^+W^- \to \bar{t}c + t\bar{c}$, and we calculate the single-top/single-charm production rate at the LHC. The rates are such that the background from single-top/single-bottom production will probably swamp the signal.

1

1   Introduction

It has now been established that the mass of the top quark is well above 163 GeV. This makes the decay $t \rightarrow c\, W^+W^-$ kinematically accessible. The branching ratio for this decay in the Standard Model was studied by Jenkins[1]. The diagram is given in Figure 1, where the internal fermion can be any of the charge $-1/3$ quarks. Jenkins showed that the rate is extremely small. There are two reasons for this. The first, of course, is phase space. The second is a GIM cancellation, which makes the resulting rate proportional to the square of the b-quark mass. Jenkins noted that this second suppression might be absent in other models, and that in these models the rate might be measurable.

In this letter, we first look at the decay $t \rightarrow c\, W^+W^-$ in a very generic set of models, in which the exchanged particle can be either a scalar, a fermion or a vector boson. We then note that in any model in which the decay $t \rightarrow c\, W^+W^-$ occurs, one will also have the process $W^+W^- \rightarrow c\bar{t} + t\bar{c}$. This process will not be phase-space suppressed, and could thus be much larger. We will calculate the rate for $p\, p \rightarrow W^+W^- \rightarrow c\bar{t} + t\bar{c}$ for the same set of models.[1]

In section 2, we discuss the generic set of models that will be considered. The rate for $t \rightarrow c\, W^+W^-$ in these models will be calculated in section 3, and the rate for $p\, p \rightarrow W^+W^- \rightarrow c\bar{t} + t\bar{c}$ will be determined in section 4. Section 5 contains a discussion of the results and conclusions.

2   Models

The most general set of operators involving a t, c, W^+ and W^- will have 36 coefficients, each an arbitrary function of the appropriate Mandelstam variables. Rather than try to deal with this large set, we will restrict the discussion to models in which the $t \rightarrow c\, W^+W^-$ and $W^+W^- \rightarrow c\bar{t}+t\bar{c}$ processes can occur at tree-level. This seems reasonable; the rates are already very small, and in models in which these processes arise from loops and higher-dimensional operators, one would expect the rates to be even smaller. Thus, for example, the coupling of a fermion to the W-bosons will be taken to be the most general combination of V and A but not T, since tensor couplings generally arise from loops. Other than that restriction, the models will be completely general; the exchanged particle can either be a scalar, fermion or vector boson.

One of the simplest extensions of the standard model is the two-Higgs model, in which an additional scalar doublet is included. In general, such an extension will have tree-level flavor-changing neutral currents. One can avoid such currents[3] by either coupling all of fermions to one doublet, or by coupling the charge 2/3 quarks to one doublet and the charge $-1/3$ quarks to the other. This can be done via a discrete symmetry. However, it has been pointed out[4] that there is no phenomenological need to do this, as long as the

---

[1]The related process $e^+e^- \rightarrow c\bar{t} + t\bar{c} + \nu\bar{\nu}$ as well as the rate for $t \rightarrow c\, W^+W^-$, in the particular case of scalar exchange, has been calculated by Bar-Shalom et al.[2]

couplings of the scalars to the light quarks is small. From an analysis of mass matrices, Cheng and Sher[4] argued that the most natural value for the flavor-changing couplings of the neutral scalars to fermions is the geometric mean of the Yukawa couplings of the fermions, i.e. the top-charm-scalar coupling should be of $O(\sqrt{(g_Y)_t(g_Y)_c})$, where g_Y is the conventional Yukawa coupling. From this ansatz, one finds that the lower bound on the exchanged scalar mass is fairly weak, of $O(100-300)$ GeV (the precise bound depends on the amount of fine-tuning one is willing to tolerate). We will scale the top-charm-scalar coupling constant by this factor.

The diagram for scalar exchange is given in Figure 2. We have left the coupling arbitrary. As discussed above, the most natural value for a and b is $O(1)$, although in principle they could be larger (perturbation theory would become questionable if they were much larger than $O(10)$). Since the Higgs-W^+-W^- coupling depends on the Higgs vacuum expectation value, one expects C_w to be a ratio of vacuum values, i.e. of $O(1)$.

The diagram for fermion exchange is given in Figure 1. In the standard model, we expect $\alpha = \alpha' = -1$, and the contributions of the d,s and b quarks all cancel in the massless limit, leading to a result that the diagram is GIM suppressed. If there is a fourth generation, however, the internal fermion must be heavy.

The diagram for vector exchange is given in Figure 3. Here, we expect the contribution to be small. In order to interact with two W's, the neutral vector boson must mix with the Z-boson. Since the properties of the Z are in stunning agreement with theoretical expectations, any such mixing must be very small. In a wide range of models[5], the mixing must be much less than 0.01, and thus we expect the effective coupling, g_1, to be less than one percent of the weak gauge coupling. The coupling g_2 can be large, but the mass of the vector boson must be greater than 170 GeV to avoid dominating top decays.

We now turn to the calculation of $t \rightarrow c\,W^+W^-$ in these models.

3 $t \rightarrow c\,W^+W^-$

The top quark mass is known to be between (approximately) 170 and 180 GeV. In order to get the largest plausible value for the branching ratio for $t \rightarrow c\,W^+W^-$, we will take it to be 180 GeV. The differential decay rate is given by

$$\frac{d\Gamma}{dE_+dE_-} = \frac{|\mathcal{M}|^2}{64\pi^3 M_t} \tag{1}$$

where $E_\pm$ are the energies of the emitted $W^\pm$. Dividing by the standard model decay rate of the top quark, which to within a few percent is given by $G_F M_t^3/(8\pi\sqrt{2})$, gives the branching ratio, after integrating over $E_\pm$. For each of the models discussed above, we will give the square of the matrix element, and plot the resulting branching ratio. The polarizations of the final state W's will be summed over, and the charmed quark mass will be set equal to zero, except when it appears as a parameter in the scalar Yukawa coupling.

For the model with scalar exchange, shown in Figure 2, the matrix element squared is given by

$$|\mathcal{M}|^2 = \frac{g^4 M_t M_c C_w^2 (a^2 + b^2)}{(s - M_s^2)^2 + \Gamma_S^2 M_s^2} p_t \cdot p_c \left[\left(\frac{s}{2m_W^2} - 1 \right)^2 + 2 \right] \tag{2}$$

where $p_t \cdot p_c = M_t(M_t - E_+ - E_-)$ and $s = M_t(2E_+ + 2E_- M_t)$. For the scalar width, we use the expression of Atwood et al.[6], and include the effects of $S \to WW^*$ (which has a small but noticeable effect for M_s very near $2m_W$) Inserting into the expression for the branching ratio gives the result in Figure 4. There, we have taken $C_w^2(a^2 + b^2) = 1$.

One can see the resonance where the scalar mass is between $2m_W$ and M_t. In this region, the scalar can be on-shell, leading to a much larger rate. In this case, the decay would be clearly measureable. Outside of the resonance region, however, the rate falls very rapidly.[2]

The diagram for fermion exchange is given in Figure 1. The minimum value for the fermion mass, M_f, is 130 GeV. If we define $a = 1 + \alpha\alpha'$; $b = \alpha + \alpha'$; $a' = 1 - \alpha\alpha'$ and $b' = \alpha - \alpha'$, then the matrix element squared can be written as

$$|\mathcal{M}|^2 = \frac{g_1^2 g_2^2 |V_{cf}|^2 |V_{ft}|^2}{4(k^2 - M_f^2)^2} \left(M_t^2(a^2 + b^2) T_1 + M_f^2(a'^2 + b'^2) T_2 - M_f M_t(aa' + bb') T_3 \right) \tag{3}$$

where $k^2 = M_t^2 + m_W^2 - 2M_t E_+$. Note that in the standard model, $\alpha = \alpha' = -1$, so $a = -b = 2$ and $a' = b' = 0$, thus the T_2 and T_3 contributions vanish. The contributions are

$$
\begin{aligned}
T_1 &= \tfrac{1}{4w^2}\Big[4w^2 + 5w - 3w^3 - 5xw^2 + 3x - 11xw + 3w^3x - 16x^2 \\
&\quad -4x^2w + 28x^3 + 12x^3w - 16x^4 - 2yw^2 - 5yw + 3w^3y \\
&\quad -2xyw^2 - 2xy + 12xyw + 8x^2y - 4x^2yw - 8x^3y \Big]
\end{aligned}
\tag{4}
$$

where $w \equiv m_W^2$, $x = E_+$, $y = E_-$ and we have chosen units where $M_t = 1$,

$$
\begin{aligned}
T_2 &= \tfrac{1}{4w^2}\Big[w^2 - w^2x - x - wx + 4x^2 + 4wx^2 - 4x^3 \\
&\quad -w^2y + wy + 2xy - 4wxy - 4x^2y \Big]
\end{aligned}
\tag{5}
$$

and

$$T_3 = \frac{1}{4w^2}\Big[-11w^2 - 3w + 26w^2x + 12wx - 12wx^2 - 4w^2y \Big] \tag{6}$$

The results for the branching ratio, where we have set g_1 and g_2 to be the electroweak coupling, and $|V_{cf}| = |V_{ft}| = 1$ are given in Figure 5. The solid curve is the contribution

---

[2]This resonance region was also noted in the work of Bar-Shalom, et al.[2]. Our result for this decay is in agreement with theirs.

from T_1 (choosing $a^2 + b^2 = 1$), the dashed curve is the contribution from T_2 (choosing $a'^2 + b'^2 = 1$) and the dotted curve is the contribution from T_3 (choosing $aa' + bb' = 1$). Note that T_3 is defined so that the contribution to the square of the matrix element is negative; it is an interference term and we have verified that the total rate is always positive. Although we have assumed that the V_{cf} and V_{ft} KM matrix elements are unity (and the cross section obviously scales as the square of each), they are constrained somewhat by the unitarity of the KM matrix. These constraints are quite weak, giving $|V_{cf}| < 0.6$ and V_{ft} is essentially unconstrained. (Should the value of $|V_{cf}|$ be a small as one generally expects for mixing across two generations, then the branching ratio would be several orders of magnitude smaller.) Note that the resulting branching ratio is very small, generally much less than a part in 10^5. For light masses, the branching ratio increases as one approaches the resonance region (between $m_c + m_W$ and $m_t - m_W$), but the current lower bound on the mass eliminates the possibility that the heavy fermion is in that region.[3] Thus, in the case of fermion exchange, it appears that the process $t \rightarrow c\,W^+W^-$ will not be measureable, unless $|V_{cf}|$ is surprisingly large and the heavy fermion has a mass very near its current lower bound.

For vector exchange, the diagram is given in Figure 3. The expression for the square of the matrix element is

$$|\mathcal{M}|^2 = \frac{2g_1^2 g_2^2 (1+\alpha^2)}{w^2 (s - M_V^2)^2} [w^2 - \tfrac{1}{4} - 12w^3 - 19xw^2 + \tfrac{7x}{4} + \tfrac{7y}{4} + 12xw^3$$

$$+ 24x^2 w^2 - 4x^2 + 14x^2 w + 3x^3 - 12x^3 w - 19yw^2$$

$$- 4xw - 4yw + 12w^3 y + 24xyw^2 - 10xy + 20xyw$$

$$+ 17x^2 y - 20x^2 yw - 8x^3 y + 24y^2 w^2 - 4y^2 + 14y^2 w$$

$$+ 17xy^2 - 20xy^2 w - 16x^2 y^2 + 3y^3 - 12y^3 w - 8xy^3]$$

$$(7)$$

where $w \equiv m_W^2$, $x = E_+$, $y = E_-$ and we have chosen units where $M_t = 1$. Putting this expression into the branching ratio gives the result in Figure 6. Here, we have expressed the results obtained by setting $g_1^2 g_2^2 (1 + \alpha^2) = 1$. As discussed in section 2, however, one expects g_2 to be two orders of magnitude less than the weak gauge coupling, so as not to significantly mix with the Z. Thus, g_2^2 is at most 10^{-5}, and thus the decay is unmeasureable.

Part of the reason that these decay rates are so small is simply phase space. Any model with $t \rightarrow c\,W^+W^-$ will also have $W^+W^- \rightarrow c\bar{t} + t\bar{c}$ and one could look for single-top/single-charm production in hadron colliders. Such a process will not be phase-space suppressed and might be much larger. We now turn to this process.

---

[3]D0 has quoted[7] a firm lower bound of $m_Z + m_b$ on the mass; from their data it appears that a 2σ lower bound would be approximately $110 - 120$ GeV.

4 $W^+W^- \rightarrow c\bar{t} + t\bar{c}$

In order to relate a process involving W^+W^- scattering to a process involving pp scattering, one needs to know the W content of the proton. We follow the procedure of Johnson, Olness and Tung.[8] The cross section is

$$\sigma(pp \rightarrow WW) = \int dy_1 dy_2 dz_1 dz_2 \, f_W^d(z_1) f_d^p(y_1) f_W^u(z_2) f_u^p(y_2) \hat{\sigma}(z_1 z_2 y_1 y_2 s) \tag{8}$$

where, for example, f_W^d is the W content of the down quark. Changing variables to $x_1 \equiv y_1 z_1, \; x_2 \equiv y_2 z_2$ and defining $\tau \equiv x_1 x_2$, this can be written as

$$\sigma = \int \mathcal{L}(\tau) \hat{\sigma}(\tau s) d\tau \tag{9}$$

where

$$\mathcal{L}(\tau) = \int_\tau^1 \frac{1}{x_1} f_{W^-}^p(x_1) f_{W^+}^p(\frac{\tau}{x_1}) \, dx_1 \tag{10}$$

Here

$$f_{W^-}^p(x_1) = \int_{x_1}^1 \frac{1}{y_1} f_{W^-}^d(x_1/y_1) f_d^p(y_1) dy_1 \tag{11}$$

with a similar expression for $f_{W^+}^p(x_2)$. Since the structure functions have been previously calculated (see Ref. 8), $f_{W^-}^p$ and $f_{W^+}^p$ can be determined initially, and then only the single integral for σ above needs to be done. It is important to note that structure functions for longitudinal W's differ from those of transverse W's, and thus the scattering cross sections must be determined for every combination

The cross section is given by

$$\hat{\sigma} = \frac{|\mathcal{M}|^2}{16\pi s} \frac{1 - M_t^2/s}{\sqrt{1 - 4m_W^2/s}} \tag{12}$$

and thus we only need to determine the matrix elements squared for each process. We will designate the transverse W's as W_L and W_R, and the longitudinal W as W_0.

For the scalar exchange diagram, the only nonzero contributions are $W_L W_L$, $W_R W_R$ and $W_0 W_0$. For $W_L W_L$ and $W_R W_R$, the square of the matrix element is

$$|\mathcal{M}|^2 = \frac{g^4 M_t M_c C_w^2 (a^2 + b^2)}{(s - M_s^2)^2 + \Gamma_S^2 M_s^2} (s - M_t^2) \tag{13}$$

and for $W_0 W_0$ it is

$$|\mathcal{M}|^2 = \frac{g^4 M_t M_c C_w^2 (a^2 + b^2)}{(s - M_s^2)^2 + \Gamma_S^2 M_s^2} (s - M_t^2) \left(\frac{s}{2m_W^2} - 1 \right)^2 \tag{14}$$

For the fermion exchange diagram, there are many more spin combinations. The full expressions are given in the Appendix. For the vector exchange diagram, the only

6

non-vanishing contributions are $W_L W_L$ (which is identical to $W_R W_R$), $W_L^+ W_0^-$ (which is identical to $W_R^- W_0^+$) and $W_0 W_0$. For $W_L W_L$, we find

$$|\mathcal{M}|^2 = \frac{g_1^2 g_2^2}{(s - M_V^2)^2} \frac{(1 + \alpha^2)(s - M_t^2)(s - 4m_W^2)(M_t^2 + 2s)}{3s} \tag{15}$$

For $W_L^+ W_0^-$, we have the same expression multiplied by $s/2m_W^2$, and finally, for $W_0 W_0$, we have the same expression multiplied by $(s/2m_W^2 + 1)^2$.

5 Results and Discussion

The results are given in Fig. 7. Results are given for the LHC ($\sqrt{s} = 14$ TeV). We see that the cross sections are all quite small, never exceeding 10^{-3} picobarns. Note that we have assumed that the scalar boson flavor changing coupling to the top and charm is the geometric mean of the top and charm Yukawa couplings; if it were the top Yukawa coupling, the rate could be 0.1 picobarns. Note also that we have scaled the cross-section in the case of vector exchange by $C_w^2 = 10^{-4}$, corresponding to the model-dependent bound on mixing with the Z; should mixing with the Z be suppressed, this coupling could be larger.

Could such a cross section lead to measureable single-top/single-charm production? After all, a 10^{-3} picobarn cross section, with an integrated luminosity of 1000 inverse femtobarns (possible at the LHC after several years of running), will lead to 1000 events. However, there will be a background from single-top/single-bottom production. The cross section for $pp \rightarrow q\bar{q} \rightarrow t\bar{b}$, through s-channel W-exchange, is 10 picobarns at the LHC[9] (the cross section for single top production through gluon-W fusion is larger, but the b is much softer and appropriate kinematic cuts can suppress this signal). Thus, one would have to be able to distinguish a $\bar{c}$ in a sample of 10^4 $\bar{b}$'s. Alhough kinematic cuts and good vertex detection would help, and the expected single-top/single-bottom cross section can be calculated to a few percent accuracy, it is hard to imagine that an unambiguous signal could be detected. It may not be hopeless in the scalar exchange case if the coupling of the scalar was unexpectedly large; the rate could then be as high as 0.1 picobarns, and one would get a $\bar{c}$ for every hundred $\bar{b}$'s. In this case, the signal possibly could be extracted.

In view of our statements in the introduction, the fact that $W^+ W^- \rightarrow c\bar{t} + t\bar{c}$ appears to be too small (for the most natural values of couplings) to be detected, while $t \rightarrow c W^+ W^-$ can, in some cases, be detected, may be surprising. After all, the latter does have a significant phase space suppression, while the former does not. However, the latter also has the possibility of a resonance for some mass range, while this resonance is absent in the hadronic collisions.

We conclude that the process $W^+ W^- \rightarrow c\bar{t} + t\bar{c}$ is probably undetectable at the LHC. The only hope would occur if the exchanged scalar boson had a surprisingly large coupling. The process $t \rightarrow c W^+ W^-$ may be detectable in two cases: (a) With scalar

exchange and the scalar mass between $2m_W$ and approximately 200 GeV and (b) with a heavy fermion with a mass very near the current lower bound and with an unexpectedly high mixing with the second and third generations.

6   Appendix

Here, we give the results for the fermion exchange diagram in terms of the scattering angle. Integrating over this angle is straightforward. We define $r \equiv \cos^2 \frac{\theta}{2}$ and $\bar{r} \equiv \sin^2 \frac{\theta}{2}$, and also define $K_o \equiv g^4 |V_{tf} V_{cf}^*|^2 / (t - m_F^2)^2$. Results are given for all possible combinations of α and α' equal to ± 1; other cases may be derived from those.

For $W_L W_L$ scattering, the square of the matrix element is $K_o s^{-2} (s - M_t^2) A$, where for $(\alpha, \alpha') = (1, 1)$, $A = (s - M_t^2)^2 r \bar{r}^2 (M_t^2 r + s\bar{r})$; for $(\alpha, \alpha') = (1, -1)$, $A = m_F^2 \bar{r} (M_t^2 r + s\bar{r})$; for $(\alpha, \alpha') = (-1, 1)$, A is the same with $r \leftrightarrow \bar{r}$, and for $(\alpha, \alpha') = (-1, -1)$, $A = \bar{r}(M_t^2 r + s\bar{r})(M_t^2 \bar{r} + sr)^2$. For $W_R W_R$ scattering, the result is the same

For $W_R^+ W_L^-$ scattering, only the $\alpha = \alpha'$ contributions are nonzero. For $(\alpha, \alpha') = (1, 1)$, the square of the matrix element is $K_o s^{-2} (s - M_t^2)^3 r^2 \bar{r} (\bar{r} M_t^2 + rs)$ and for $(\alpha, \alpha') = (-1, -1)$ it is the same with $r \leftrightarrow \bar{r}$. For $W_L^+ W_R^-$, the result is also the same.

For $W_0^+ W_L^-$, the square of the matrix element is $\frac{1}{2} K_o s^{-2} (s - M_t^2) m_W^{-2} (s\bar{r} + M_t^2 r) A$, where for $(\alpha, \alpha') = (1, 1)$, $A = s(s - M_t^2)^2 \bar{r} r^2$; for $(\alpha, \alpha') = (-1, +1)$, $A = s^2 r M_F^2$ and for $(\alpha, \alpha') = (-1, -1)$, $A = \bar{r}(s\bar{r} + M_t^2 r)^2$. For the remaining case, $(\alpha, \alpha') = (1, -1)$, the result vanishes. Again, for $W_0^+ W_R^-$, the result is the same.

For $W_0^- W_R^+$, the square of the matrix element is $\frac{1}{2} K_o s^{-2} (s - M_t^2) m_W^{-2} (sr + M_t^2 \bar{r}) A$, where for $(\alpha, \alpha') = (1, 1)$, $A = s(s - M_t^2)^2 r^3$; for $(\alpha, \alpha') = (1, -1)$, $A = s^2 \bar{r} M_F^2$ and for $(\alpha, \alpha') = (-1, -1)$, $A = \bar{r}^2 r$. For the remaining case, $(\alpha, \alpha') = (-1, 1)$, the result vanishes. Again, for $W_0^- W_L^+$, the result is the same.

Finally, for $W_0 W_0$, the square of the matrix element is $\frac{1}{4} K_o m_W^{-4} (s - M_t^2)(s\bar{r} + M_t^2 r) A$. For $\alpha = \alpha'$, $A = (s - M_t^2)^2 r \bar{r}^2$ and for $\alpha = -\alpha'$, $A = s m_F^2 \bar{r}$.

References

[1] E. Jenkins, Phys. Rev. D56 (1997) 458.

[2] S. Bar-Shalom, G. Eilam, A. Soni and J. Wudka, UCRHEP-T-185, hep-ph/9703221.

[3] S.L. Glashow and S. Weinberg, Phys. Rev. D15 (1977) 1958.

[4] T.P. Cheng and M. Sher, Phys. Rev. D35 (1987) 3484.

[5] P. Langacker and M. Luo, Phys. Rev. D45 (1992) 278.

[6] D. Atwood, L. Reina and A. Soni, Phys. Rev. D55 (1997) 3156.

[7] S. Abachi et al., D0 Collaboration, Phys. Rev. Lett. 78 (1997) 3819.

[8] P.W. Johnson, F.I. Olness and W.K. Tung, Phys. Rev. D36 (1987) 291.

[9] M.C. Smith and S.S. Willenbrock, Phys. Rev. D54 (1996) 6696.

FIGURE CAPTIONS

Fig. 1 This process gives $t \rightarrow c\,W^+W^-$ in the standard model, where F is any $Q = -1/3$ quark. In generic non-standard models, F is a heavy quark. We define the upper vertex to be $ig_1\gamma_\mu(1 + \alpha\gamma_5)/2\sqrt{2}$ and the lower to be $ig_2\gamma_\nu(1 + \alpha'\gamma_5)/2\sqrt{2}$.

Fig. 2 Scalar exchange contribution to $t \rightarrow c\,W^+W^-$ in a multi-scalar model. The Yukawa coupling is defined to be $-i(a+b\gamma_5)g\sqrt{m_c m_t}/\sqrt{2}m_W$ and the scalar-vector-vector coupling is defined to be $igm_W g_{\mu\nu}C_w$.

Fig. 3 Vector exchange contribution to $t \rightarrow c\,W^+W^-$. The Yukawa coupling is defined to be $ig_2\gamma_\rho(1 + \alpha\gamma_5)/2$ and the triple-vector coupling is defined to be $g_1(g_{\mu\nu}(k - p)_\rho + g_{\nu\rho}(p-q)_\mu + g_{\rho\mu}(q-k)_\nu)$, where all momenta are defined to flow outward from the vertex.

Fig. 4 Branching ratio for $t \rightarrow c\,W^+W^-$ due to non-standard model scalar exchange, using the vertices from Figure 2. The rate is proportional to $C_w^2(a^2 + b^2)$, which we have set equal to unity in the figure.

Fig. 5 Branching ratio for $t \rightarrow c\,W^+W^-$ due to heavy fermion exchange. The solid (dashed, dotted) curve is the contribution from T_1 (T_2,T_3), defined in Eq. 3. Here, we have set g_1 and g_2 equal to the electroweak gauge coupling, and set $|V_{cf}|$ and $|V_{ft}|$ equal to unity; the branching ratio scales with these quantities as shown in Eq. 3.

Fig. 6 Branching ratio for $t \rightarrow c\,W^+W^-$ due to non-standard model vector exchange, using the vertices from Figure 3. In plotting the above, we have set $g_1^2 g_2^2(1 + \alpha^2)$ equal to unity. As discussed in the text, in most models limits from mixing with the standard model Z force g_1 to be roughly two orders of magnitude smaller than the gauge coupling; the branching ratio in such a case will be more than four orders of magnitude smaller than shown in the figure.

Fig. 7 Cross section for $W^+W^- \rightarrow c\bar{t} + t\bar{c}$ at the LHC ($\sqrt{s} = 14$ TeV). For vector exchange indicated by the dashed line, the value of C_w^2 has been taken to be 10^{-4}, which is the maximum value expected from limits on Z mixing. The solid line corresponds to scalar exchange, The other lines indicate the cross section for fermion exchange. The labels $\{LL,\ LR,\ RL,\ RR\}$ refere to the cases where (α, α') are $\{(-1,-1),\ (-1,+1),\ (+1,-1),\ (+1,+1)\}$ respectively.
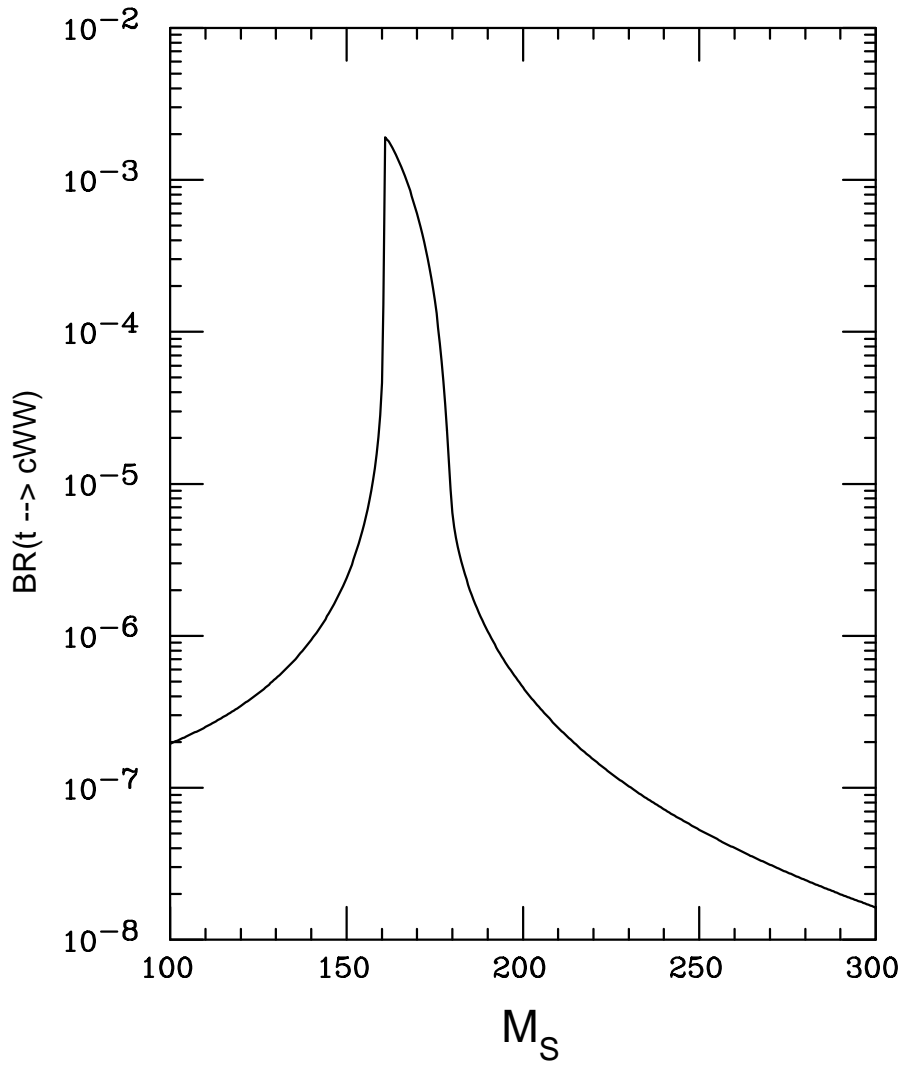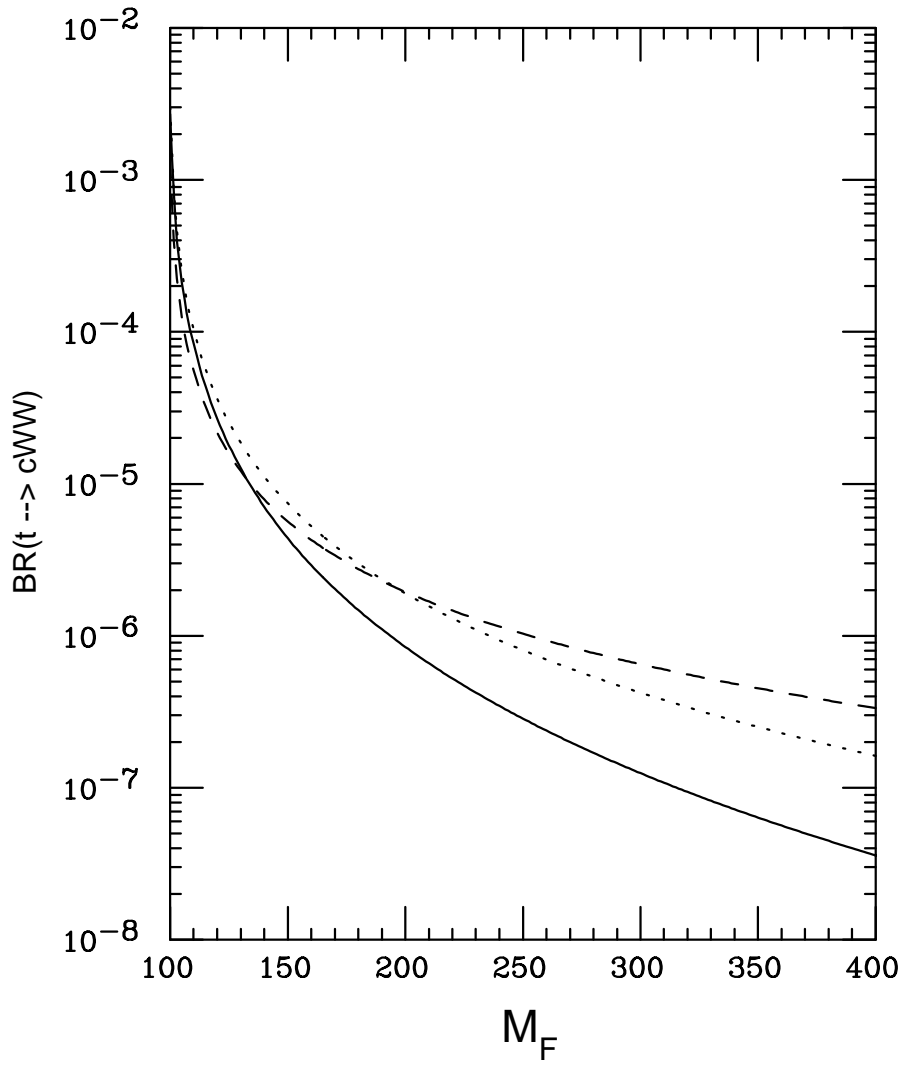
Figure 4

Figure 5

Figure 6

Figure 7
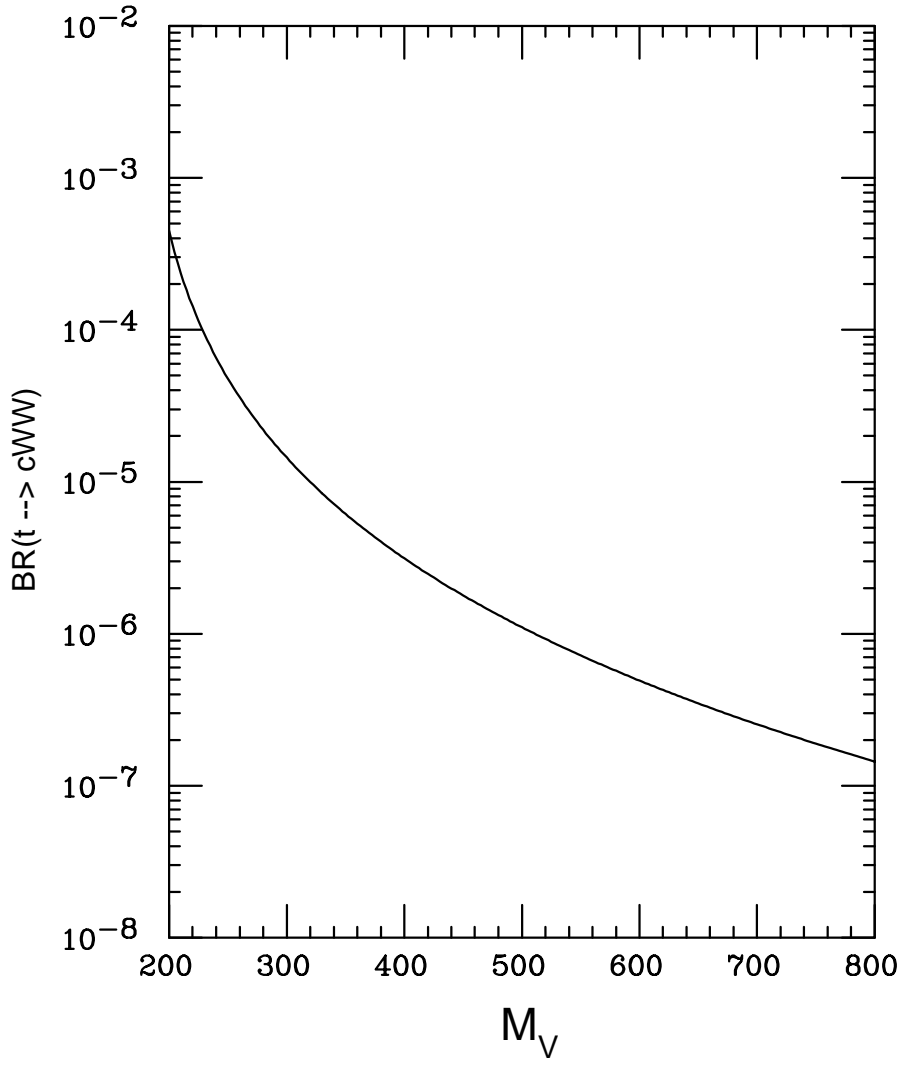
17